Zoi Michailidou,[1,2] Nicholas M. Morton,[2] José Maria Moreno Navarrete,[3] Christopher C. West,[4] Kenneth J. Stewart,[5] José Manuel Fernández-Real,[3] Christopher J. Schofield,[6] Jonathan R. Seckl,[2] and Peter J. Ratcliffe[1]

Adipocyte Pseudohypoxia Suppresses Lipolysis and Facilitates Benign Adipose Tissue Expansion

Diabetes 2015;64:733–745 | DOI: 10.2337/db14-0233

Prolyl hydroxylase enzymes (PHDs) sense cellular oxygen upstream of hypoxia-inducible factor (HIF) signaling, leading to HIF degradation in normoxic conditions. In this study, we demonstrate that adipose PHD2 inhibition plays a key role in the suppression of adipocyte lipolysis. Adipose *Phd2* gene ablation in mice enhanced adiposity, with a parallel increase in adipose vascularization associated with reduced circulating nonesterified fatty acid levels and normal glucose homeostasis. *Phd2* gene–depleted adipocytes exhibited lower basal lipolysis in normoxia and reduced β-adrenergic–stimulated lipolysis in both normoxia and hypoxia. A selective PHD inhibitor suppressed lipolysis in murine and human adipocytes in vitro and in vivo in mice. PHD2 genetic ablation and pharmacological inhibition attenuated protein levels of the key lipolytic effectors hormone-sensitive lipase and adipose triglyceride lipase (ATGL), suggesting a link between adipocyte oxygen sensing and fatty acid release. *PHD2* mRNA levels correlated positively with mRNA levels of AB-hydrolase domain containing-5, an activator of ATGL, and negatively with mRNA levels of lipid droplet proteins, perilipin, and TIP47 in human subcutaneous adipose tissue. Therapeutic pseudohypoxia caused by PHD2 inhibition in adipocytes blunts lipolysis and promotes benign adipose tissue expansion and may have therapeutic applications in obesity or lipodystrophy.

In obesity, the gradual expansion of adipose tissue associates with local hypoxia due to an inadequate vascular response (1,2). Hypoxic adipose tissue, as found in diet-induced obesity models, or transgenic hypoxia-inducible factor (HIF)-1α overexpression in adipose tissue associates with local inflammation, fibrosis, and metabolic dysfunction (1–6). In contrast, in models of dietary obesity in which adipose tissue hypoxia is attenuated (11β-HSD1–deficient mice and transgenic adipose overexpression of vascular endothelial growth factor [VEGF]), the structural and metabolic abnormalities are ameliorated, and benign adipose tissue expansion occurs (7–10). Understanding mechanisms that allow benign expansion of adipose depots is of high importance, as it may lead to therapeutic strategies for minimizing the pathogenesis of obesity and/or lipodystrophy syndromes.

Critical for benign expansion of fat depots is efficient storage and release of fatty acids in adipocytes (11,12) and adequate expandability of the adipose–vascular network (13). Adipose tissue expansion is a dynamic process that involves adipocyte hypertrophy in combination with vascular remodeling involving endothelial cells, macrophages, and the extracellular matrix (13–16). Low oxygen tension (hypoxia) can occur due to an inability of the tissue to provide adequate compensatory vascular supply (1–5). In this context, cells respond to hypoxia by activation and stabilization of the HIFα isoforms (17). Increased HIF-1α

[1]Henry Wellcome Building for Molecular Physiology, University of Oxford, Oxford, U.K.
[2]University of Edinburgh/British Heart Foundation Centre for Cardiovascular Science, Queen's Medical Research Institute, Edinburgh, U.K.
[3]CIBERobn "Pathophysiology of Obesity and Nutrition," Biomedical Research Institute of Girona (IDIBGI), Girona, Spain
[4]University of Edinburgh/MRC Centre for Regenerative Medicine, Edinburgh, U.K.
[5]The Department of Plastic, Reconstructive and Burns Surgery, St. Johns Hospital, Livingston, U.K.
[6]Chemistry Research Laboratory, Oxford University, Oxford, U.K.

Corresponding author: Zoi Michailidou, v1zmicha@staffmail.ed.ac.uk.

Received 11 February 2014 and accepted 10 September 2014.

This article contains Supplementary Data online at http://diabetes.diabetesjournals.org/lookup/suppl/doi:10.2337/db14-0233/-/DC1.

activation may contribute to the pathological changes within adipose tissue in obesity (1–5) in part through inhibition of peroxisome proliferator-activated receptor γ-2–dependent adipogenesis (18). This concept is supported by the phenotype of transgenic mice overexpressing *Hif1α* in adipose tissue that exhibits insulin resistance and localized adipose tissue fibrosis (6). In contrast, HIF-2α promotes adipose differentiation in vitro and, given that HIF-2α levels are also increased after 4 weeks in high-fat–fed mice (19), may counteract pathogenic changes associated with HIF-1 at early stages of obesity development. The oxygen-sensitive signal event that regulates HIF is mediated by hydroxylase enzymes that regulate the protein stability and consequent transcriptional activity of HIFα (20). HIF–prolyl hydroxylases (PHDs; otherwise known as EGLNs) belong to the large family of Fe (II) and 2-oxoglutarate–dependent oxygenases (21–24). PHDs hydroxylate conserved prolyl residues of the HIF-1α and HIF-2α subunits, thus promoting their binding to the von Hippel Lindau (VHL) tumor suppressor protein, which targets HIFα isoforms for proteasomal degradation in normoxia (21–24). In humans, there are three isoforms of PHD enzymes (PHD1–3), with PHD2 (EGLN1) the most abundant enzyme, including in mature adipocytes (25). PHD2 is the most important for setting basal activity of the HIF system in most cells (20). Despite the growing understanding of the pathological role of HIF-1α activation in adipose tissue during obesity (1–10,26–32), direct pharmacological targeting of HIF remains challenging. In contrast, therapeutic targeting of PHDs to induce a pseudohypoxic (activation of HIFα and target genes in normoxia) state is under active clinical development in the context of anemia and other diseases involving hypoxia (33,34). In this study, we addressed the metabolic consequences and potential therapeutic impact of pseudohypoxia by genetic and pharmacological inhibition of the principal oxygen-sensing enzyme PHD2 in adipose tissue.

RESEARCH DESIGN AND METHODS

Animal Studies

The *Phd2* conditional allele (35) on a congenic C57BL/6J background, the *Hif1α* conditional allele (36), and the *Hif2α* conditional allele (37) were crossed with the fatty acid binding protein 4 (*Fapb4*)-*Cre* allele (38) (The Jackson Laboratory) to achieve adipose-specific conditional knockout mice. Hif1α (stock number 007561) and Hif2α (stock number 008407) mice were purchased from The Jackson Laboratory. Genotyping and recombination efficiency PCRs were performed as previously described (35–39). In all experiments described, control littermates were used for comparisons. For diet-induced obesity experiments, mice were given the D12331 high-fat diet (58% kcal fat; Research Diets Inc.) for 12 weeks. To assess the effect on adipocyte lipolysis of pharmacologically inhibiting PHD, we used 2-(1-chloro-4-hydroxyisoquinoline-3-carboxamido) acetic acid (40,41), a potent small-molecule inhibitor of the PHD enzymes that has been shown to activate HIFα (40,41). For analysis of the effects of this PHD inhibitor (PHI) in vivo, C57BL/6J mice were used. In brief, mice were fasted overnight, blood was collected for basal nonesterified fatty acid (NEFA) quantification, mice were then divided into two groups, those receiving intraperitoneal (i.p.) PHI (30 mg/kg; a dose that was sufficient to robustly induce HIF in liver) (41) and a control group receiving vehicle (5% DMSO) alone. PHI was administered for an hour prior to CL316,243 (1 μg/kg) stimulation. Male adult mice were used in all the experiments. Animals were bred under standard conditions and fed standard chow (product 801151; Special Diet Services, Essex, U.K.) ad libitum unless stated otherwise. Animal studies were performed under licensed approval in accordance with the U.K. Home Office Animals (Scientific Procedures) Act, 1986.

Systemic Tests and Biochemistry

For glucose tolerance tests, mice were fasted 5 h before administration of glucose (2 mg/g body weight [BW]) orally or by i.p. injection. Glucose concentration was measured by a blood glucose monitoring system (OneTouch Ultra2; LifeScan, Milpitas, CA). For β3-adrenergic receptor agonist tests, mice were fasted overnight, and blood samples were collected before and 15, 30, and 60 min after i.p. injection of 1 μg/kg CL316,243 (Sigma-Aldrich, Dorset, U.K.). In the PHI experiments, PHI was administered i.p. (30 mg/kg) and blood collected 1 h prior to the i.p. CL316,243 challenge. Insulin and leptin concentrations were measured using commercial ELISA kits (Crystal Chem Inc., Downers Grove, IL). Liver and muscle triglyceride levels were measured using a commercial kit (Abcam, Cambridge, U.K.) according to the manufacturer's instructions.

Quantitative RT-PCR

Total RNA was extracted from cells and tissue using TRIzol (Invitrogen, Paisley, U.K.) and treated with DNase I (Invitrogen). One microgram total RNA was used for first-strand DNA synthesis using SuperScript III cDNA Synthesis system (Invitrogen), and quantitative PCR (qPCR) was performed with the LightCycler 480 (Roche), using mouse TaqMan assays (Life Technologies, Paisley, U.K.) for all genes measured. A standard curve was constructed for each gene measured using a serial dilution of cDNA pooled from all samples. Results were normalized to the expression of 18S rRNA.

Immunoblot Assays

Whole-cell lysates were prepared in ice-cold buffer (5 mmol/L HEPES, 137 mmol/L NaCl, 1 mmol/L $MgCl_2$, 1 mmol/L $CaCl_2$, 10 mmol/L NaF, 2 mmol/L EDTA, 10 mmol/L Na pyrophosphate, 2 mmol/L Na_3VO_4, 1% Nonidet P-40, and 10% glycerol) containing protease inhibitors (Complete Mini; Roche Diagnostics Ltd., West Sussex, U.K.). Blots were probed with HIF-1α (Cayman Chemical, Ann Arbor, MI), HIF-2α (Novus Biologicals, Littleton, CO), and HIF PHD2 (Novus Biologicals) antibodies. Lipolysis activation antibody kit was used to

identify hormone-sensitive lipase (HSL), phosphorylated (p-)HSL^{660}, p-HSL^{565}, and perilipin (New England BioLabs, Ipswich, MA). The adipose triglyceride lipase (ATGL), AKT, and p-AKT (Ser473) antibodies were from Cell Signaling Technology (Hertfordshire, U.K). HRP-conjugated anti-rabbit (Dako, Cambridgeshire, U.K.) secondary antibody was used. Signal was detected using ECL Plus (GE Healthcare Life Sciences, Buckinghamshire, U.K.). Blots were reprobed with an HRP-conjugated anti-actin antibody (Abcam). Densitometry was performed using the ImageJ software.

Histology and Immunohistochemistry

Formalin-fixed, paraffin-embedded adipose sections (4 μm) were used. Images were acquired using a Zeiss microscope (Zeiss, Hertfordshire, U.K.) equipped with a Kodak DCS 330 camera (Eastman Kodak, Rochester, NY). Adipocyte size was calculated by measuring the diameter of adipocytes from 20 randomly selected areas per section using a Zeiss KS300 image analyzer. Antibodies to CD31 (Abcam) for endothelial cells/vessels or F4/80 (Abcam) for macrophages were used. Binding of primary antibody was visualized using diaminobenzidine, Chromogen-A (Dako). Counterstain was performed by rinsing in 70% hematoxylin. Picrosirius red (Sigma-Aldrich) staining of adipose sections was used to identify total collagen. Analysis was performed blind to the experimental grouping as previously described (7).

In Vitro Adipocyte Lipolysis Experiments

Primary murine or human adipocytes were isolated as previously described (7). For the analysis of lipolysis in aP2-*Phd2*KO, aP2-*Hif1α*KO, and aP2-*Hif2α*KO adipocytes, hypoxic stimulation was performed by replacing the media with 1% O_2 preconditioned media. Cells were left at 1% O_2 in a hypoxic chamber (1% O_2) for 4 h, after which media was collected for measurement of NEFA release, and cells were lysed in RIPA protein lysis buffer for analysis by immunoblotting. Effects of PHI on lipolysis were examined in C57BL/6J primary adipocytes. In brief, adipocytes were pretreated with PHI [0.5 mmol/L, a sufficient dose to robustly activate HIFα (41)] or vehicle (DMSO, 0.5%) for 1 h prior to β-adrenergic stimulation with CL316,243 (100 nmol/L) for 3 h. Medium was collected for measuring NEFA concentrations with a NEFA kit (Alpha Laboratories, Eastleigh, U.K.), and adipocytes were lysed for protein quantification and immunoblot analysis.

Human Adipocyte Lipolysis Studies

Human abdominal subcutaneous adipose tissue (SAT) was obtained, after written consent, from healthy female subjects (age range 30–50 years old) with mean BMI 25.6 (± 1.9) kg/m^2 undergoing cosmetic lipectomy procedures. Ethical approval for the collection of tissue and subsequent research was granted by the South East Scotland Research Ethics Committee 3, reference number 10/S1103/45. Adipocytes were isolated as above and exposed to PHI as above. In brief, human adipocytes were pretreated with PHI or vehicle 1 h prior to stimulation with isoproterenol (100 nmol/L) for an additional 2 h. Medium was collected for measuring NEFA concentrations, and adipocytes were lysed for protein quantification and immunoblot analysis.

Human Adipose Tissue Gene Expression Study

Adipose tissue samples (91 subcutaneous and 102 omental abdominal) were obtained from the same location during elective surgical procedures (cholecystectomy [n = 10], surgery of abdominal hernia [n = 14], and gastric bypass surgery [n = 78]) from participants with BMI within 20–68 kg/m^2. All subjects were of Caucasian origin and reported that their BW had been stable for at least 3 months before the study. In the obese type 2 diabetic group, two subjects were treated with metformin, one with glitazones, and one with insulin. Liver and renal diseases were specifically excluded by biochemical workup, measuring biomarkers of liver and renal injury. All subjects gave written informed consent, approved by the ethics committee (Comitè d'Ètica d'Investigació Clínica). Adipose tissue samples were immediately frozen in liquid nitrogen and stored at −80°C. RNA was prepared using RNeasy Lipid Tissue Mini Kit (Qiagen, Barcelona, Spain) and integrity checked by Agilent Bioanalyzer (Agilent Technologies, Palo Alto, CA) and reverse transcribed to cDNA using High-Capacity cDNA Archive Kit (Applied Biosystems, Madrid, Spain) according to the manufacturer's protocol. Gene expression was assessed by real-time PCR using a LightCycler 480 Real-Time PCR System (Roche Diagnostics SL, Barcelona, Spain), using commercially available TaqMan primer/probe sets (Applied Biosystems). A threshold cycle (Ct) value was obtained for each amplification curve, and a ΔCt value was first calculated by subtracting the Ct value for human *Cyclophilin A* (PPIA) RNA from the Ct value for each sample. Fold changes compared with the endogenous control were then determined by calculating $2^{-\Delta Ct}$. Results are expressed as ratio to PPIA gene expression.

Statistics

Values are reported as mean ± SEM. All statistical analysis was performed in GraphPad Prism 5 software. Simple comparisons were analyzed using Student t test. For multiple comparisons, differences between genotypes and the effect of treatment(s) were analyzed by two-way ANOVA with subsequent Tukey post hoc test or Mann–Whitney if data were not normally distributed. Significance was set at $P < 0.05$.

RESULTS

Adipose *Phd2* Deficiency Stabilizes HIFα Levels and Upregulates HIFα Target Genes

We studied intercross progeny of the littermate genotype *Phd2*$^{lox/lox}$ mice (control, designated *Phd2*; described in Refs. 35,39) with the *Fapb-4-Cre* (aP2-Cre) mice (38) to make an adipose tissue-selective *Phd2* deficiency model designated aP2-*Phd2*KO. Efficient recombination was detected in epididymal, mesenteric, and brown adipose

tissue and in isolated epididymal adipocytes (Supplementary Fig. 1*A*). Recombination was observed in the whole stromal vascular fraction, but there was no evidence for recombination in macrophages (Supplementary Fig. 1*A*). PHD2 mRNA (Fig. 1*A*) and protein were efficiently knocked down (~70%) in aP2-*Phd2*KO adipose tissue (Fig. 1*B*) and in primary adipocytes (Fig. 1*C*) cultured in vitro. No significant *Phd2* recombination was found in other tissues such as heart, muscle, spleen, or liver (Supplementary Fig. 1*B*). Adipose *Phd1* and *Phd3* mRNA levels were unaffected (Supplementary Fig. 1*C*). Hypoxia markedly upregulated *Phd2* mRNA levels in vitro (threefold; $P < 0.0001$) in control adipocytes, but this induction was absent in aP2-*Phd2*KO adipocytes (Fig. 1*D*).

Homozygous deletion of *Phd2* in adipocytes led to stabilization of HIF-1α and HIF-2α protein levels in adipose under normoxic conditions (Fig. 1*E* and *F*). HIF target genes encoding proteins for nutrient metabolism (*Glut1*, *Glut4*, *Pdk1*, and *Pdk4*) and angiogenesis (*Vegfα*, *Angptl4*, and *Tgfb*) were higher in white adipose tissue of aP2-*Phd2*KO compared with control littermates (Fig. 2*A*). Hypoxia led to significantly higher mRNA levels of *Glut1* and *Vegfα* in isolated aP2-*Phd2*KO than control adipocytes (Fig. 2*B*). In order to evaluate which *Hifα* isoform dominantly regulates target genes in the aP2-*Phd2*KO model, we measured mRNA levels of the same genes in mice with adipose-specific deletion (aP2-Cre–driven deletion) of *Hif1α* (aP2-*Hif1α*KO) or *Hif2α* (aP2-*Hif2α*KO), which blunts the hypoxia-induced stabilization of HIF-1α in adipocytes (Supplementary Fig. 2*A*). Deletion of *Hif1α* in adipose tissue reduced the mRNA levels of genes that control nutrient metabolism (*Glut1*, *Pdk1*, and *Pdk4*) and the profibrotic response (*Tgfb*), with pronounced effects in high-fat–fed animals (Fig. 2*C*). This effect was localized to mature adipocytes (Supplementary Fig. 2*B*). In contrast, adipose *Hif2α* deletion reduced the mRNA levels of angiogenic genes (*Vegfα* and *Angptl4*) (Fig. 2*D*), indicating a predominant role for HIF-2α in adipose vascularization.

Adipose *Phd2* Deficiency Increases Adiposity in Parallel With Increased Adipose Vascularization

Chow diet (low-fat)–fed aP2-*Phd2*KO mice exhibited increased adiposity by 19 weeks of age compared with control littermates (Fig. 3*A*), with approximately twofold higher cumulative weight gain from 9–30 weeks (Fig. 3*B*). Adult aP2-*Phd2*KO mice had more white adipose tissue mass (>50%) in all depots, but brown adipose and liver masses were unaltered (Fig. 3*C*). Body and adipose tissue weight differences were not due to increased food intake (Fig. 3*D*). As expected for their higher adiposity,

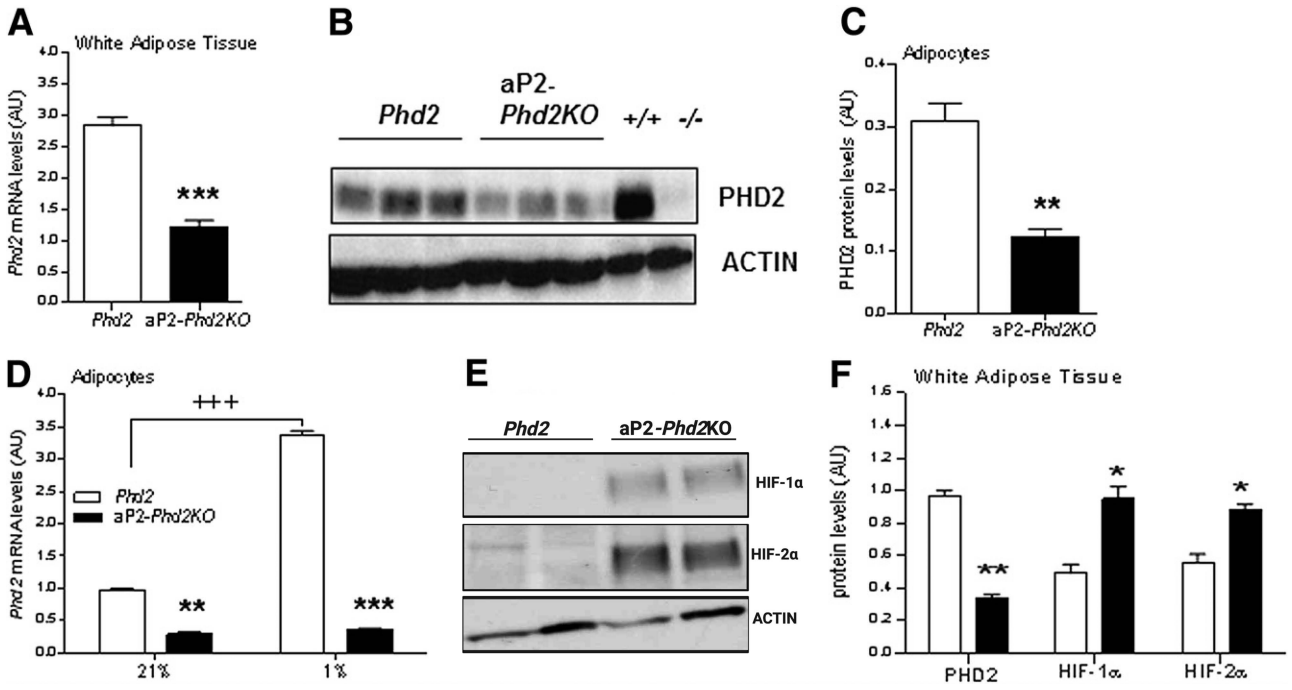

Figure 1—Efficient aP2-Cre–mediated knockdown of PHD2 in adipocytes stabilizes both HIFα isoforms. *A*: Reduced *Phd2* mRNA levels in aP2-*Phd2*KO white adipose tissue (black bars) compared with control *Phd2* littermates (white bars); $n = 5$. *B*: Representative Western blot showing reduced PHD2 protein levels (top panel, from left to right, lanes 4–6) in aP2-*Phd2*KO white adipose tissue compared with control littermates (top panel, lanes 1–3). Mouse embryonic fibroblast lysates from *Phd2* wild-type ($^{+/+}$; lane 7) and *Phd2* knockout ($^{-/-}$; lane 8) mice were included to identify specificity of the anti-PHD2 antibody. *C*: Reduced PHD2 protein levels in aP2-*Phd2*KO adipocytes. Quantification graph of a representative Western blot. *D*: Reduced *Phd2* mRNA levels in isolated aP2-*Phd2*KO adipocytes cultured in normoxia (21% O_2) and ablated response to hypoxia (1% O_2). Representative Western blots (*E*) and quantification graph (*F*) showing stabilization of both HIF-1α and HIF-2α in adipose tissue in aP2-*Phd2*KO adipose. mRNA was corrected to 18S and protein to β-actin. Data are presented as arbitrary units (AU). *$P < 0.05$, **$P < 0.01$, ***$P < 0.001$ between genotypes; +++$P < 0.001$ comparison of hypoxia and normoxia within a genotype.

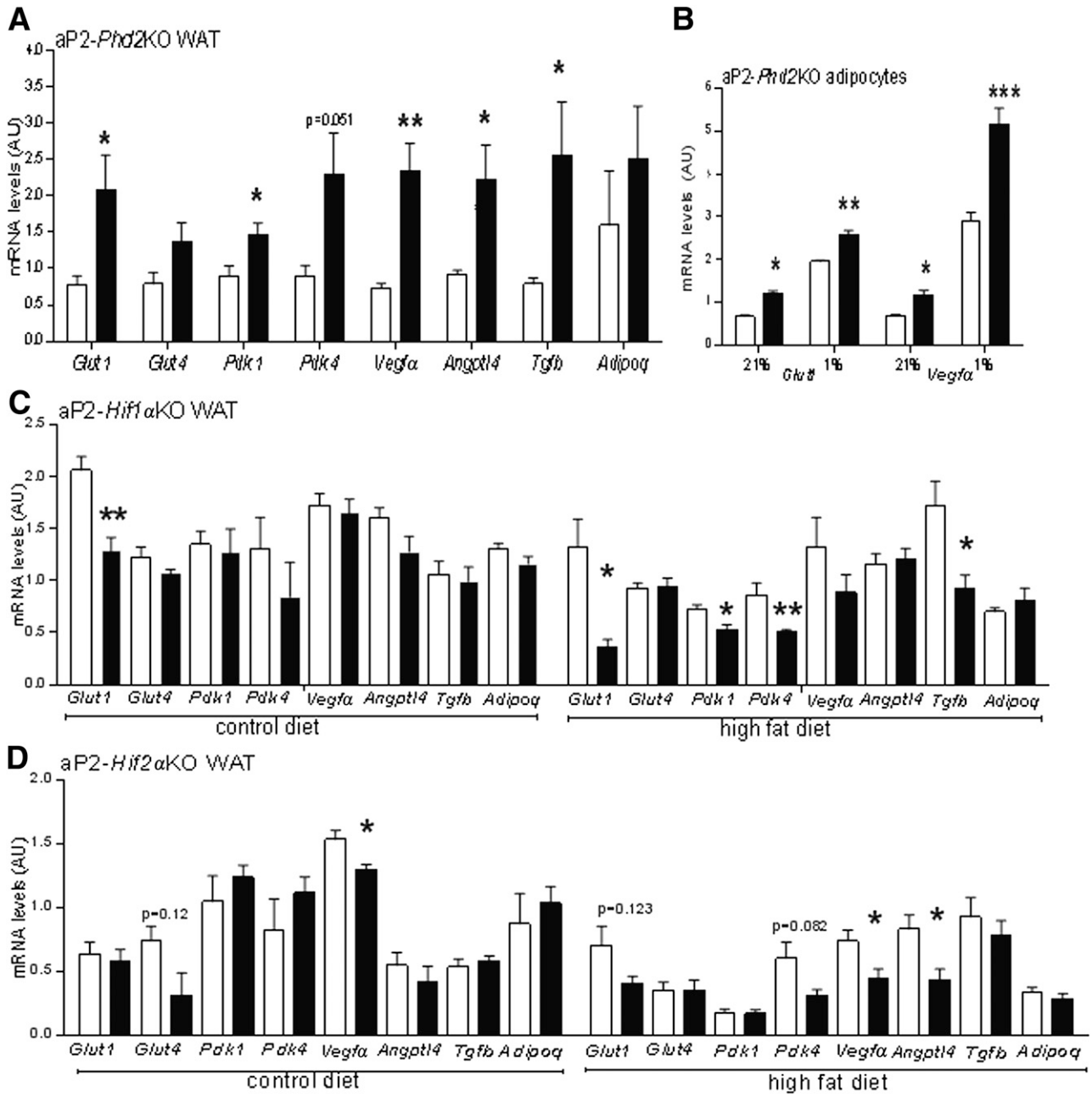

Figure 2— Adipose *Phd2* deficiency upregulates HIF target genes in normoxia. *A*: Upregulation of HIFα target genes in white adipose tissue (WAT) of aP2-*Phd2*KO mice (black bars) compared with control *Phd2* littermates (white bars); n = 7/group. *B*: Isolated aP2-*Phd2*KO adipocytes showed higher mRNA levels of *Glut1* and *Vegfα* in both normoxia (21% O_2) and hypoxia (1%; 4 h); n = 3/group. aP2-*Hif1α*KO (black bars, n = 4–11/group) (*C*) and aP2-*Hif2α*KO (black bars, n = 4–6/group) (*D*) mice with their littermate controls (white bars) were fed a control diet or a high-fat diet (58% kcal fat) for 12 weeks. mRNA levels of HIF-target genes in adipose tissue were measured and corrected to 18S; data are presented as arbitrary units (AU). *P < 0.05, **P < 0.01, ***P < 0. 001.

aP2-*Phd2*KO mice showed a parallel increase in plasma leptin levels (Table 1).

Adipose *Phd2* Deficiency Maintains Glucose Tolerance Associated With Suppressed Lipolysis and Reduced Ectopic Lipid Accumulation

Despite increased adiposity, aP2-*Phd2*KO mice exhibited normal glucose tolerance (Fig. 3*E*) and similar fasted and fed plasma insulin levels (Table 1) to their control littermates. aP2-*Phd2*KO mice had comparable ad libitum–fed but reduced fasting NEFA levels (after 5 h or overnight fast, Table 1 and Fig. 3*F*). Notably, aP2-*Phd2*KO mice exhibited blunted β-adrenergic agonist CL316,243 responsiveness in vivo (Fig. 3*F*), with significantly reduced NEFA release. Liver and muscle triglyceride levels were lower in aP2-*Phd2*KO mice (Fig. 3*G*).

Greater fat deposition in aP2-*Phd2*KO mice was associated with larger adipocytes (diameter, 230 ± 12 and 177 ± 18

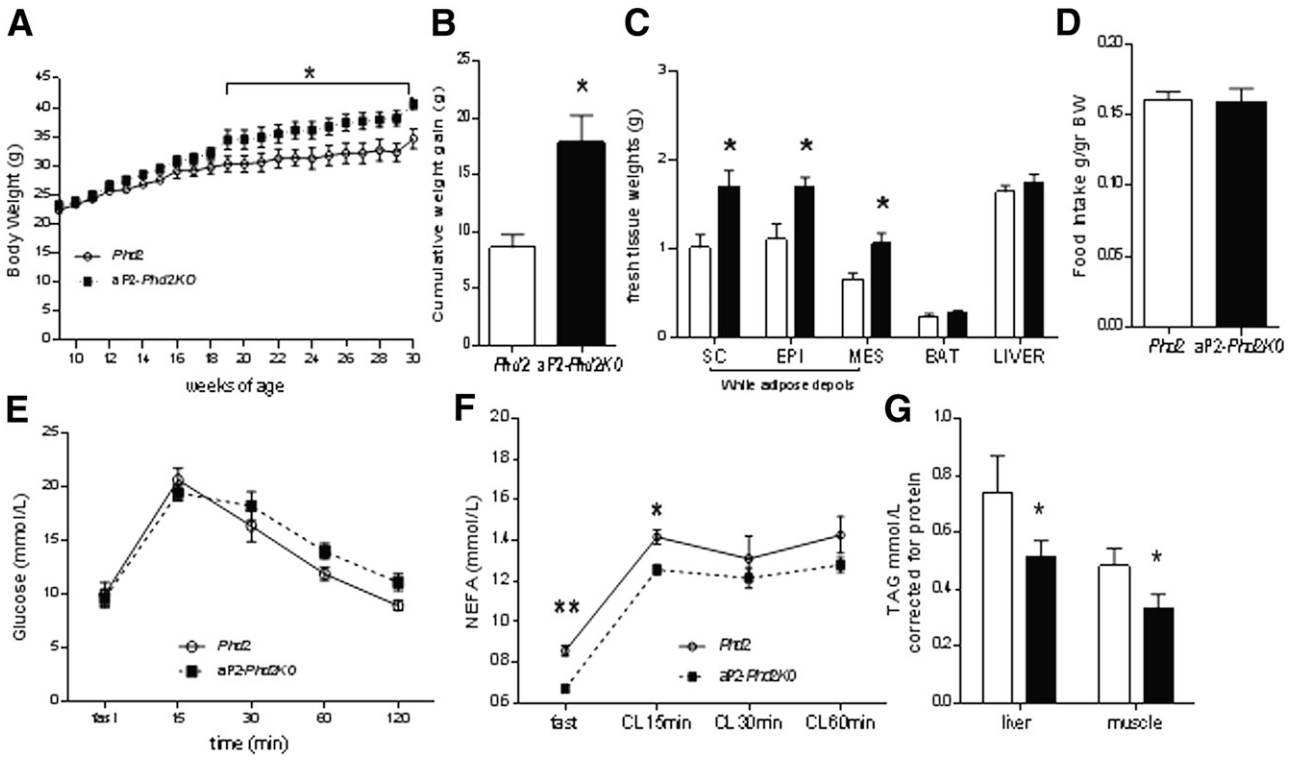

Figure 3—Adipose *Phd2*-deficient mice exhibit increased adiposity, lower plasma NEFA levels, and reduced triglyceride levels in liver and muscle. *A*: BWs in chow-fed aP2-*Phd2*KO (black squares, dashed line) are significantly higher after 18 weeks of age compared with *Phd2* control mice (open circles, solid line); $n = 7$/group. *B*: aP2-*Phd2*KO mice (black bars) gain more weight between 9 and 30 weeks of age. *C*: aP2-*Phd2*KO mice (black bars; $n = 7$) have heavier white fat depots (EPI, epididymal; MES, mesenteric; SC, subcutaneous) but similar brown adipose tissue (BAT) and liver weights to control *Phd2* littermates (white bars; $n = 5$). *D*: Short-term food intake was recorded between 14 and 16 weeks of age. There were no apparent differences in food intake between genotypes ($n = 5$/group). *E*: An i.p. glucose tolerance test (2 mg/g BW glucose) in aP2-*Phd2*KO and control littermate mice ($n = 6$/group). *F*: Circulating NEFA concentrations in aP2-*Phd2*KO mice before and after stimulation with a lipolytic β3-adrenergic agonist, CL316,243 (1 μg/g BW i.p.) ($n = 5$/group). *G*: Liver and muscle triglyceride (TAG) levels in aP2-*Phd2*KO (black bars; $n = 6$) and control littermate (white bars; $n = 8$) mice. $^*P < 0.05$ between genotypes; $^{**}P < 0.01$ between genotypes.

μm in controls; $P = 0.034$) (Fig. 4*A*). However, adipose *Phd2* deficiency did not affect adipose macrophage density (Fig. 4*B*) or fibrosis (Fig. 4*C*, Supplementary Fig. 3), markers of inflamed and hypoxic adipose tissue, respectively. Intriguingly, adipose *Phd2*-deficient mice manifested approximately twofold ($P = 0.001$) greater density of immunostaining for the endothelial marker CD31 in adipose tissue, indicating an enhanced vascular expansion (Fig. 4*D* and *E*).

Table 1—Plasma biochemistry in *Phd2* and aP2-*Phd2*KO mice

	Phd2	aP2-*Phd2*KO	*P* value
Fed insulin (ng/mL)	3.7 ± 0.8	3.8 ± 0.7	0.87
Fasted (overnight) insulin (ng/mL)	0.08 ± 0.02	0.1 ± 0.01	0.21
Fasted (5 h) insulin (ng/mL)	1.6 ± 0.2	1.6 ± 0.3	0.95
Fed leptin (ng/mL)	19.2 ± 4.0	**37.2 ± 3.7****	*0.009*
Fed NEFA (mmol/L)	0.8 ± 0.06	0.6 ± 0.09	0.23
Fasted (5 h) NEFA (mmol/L)	1.1 ± 0.09	**0.8 ± 0.04***	*0.048*

Data are mean ± SEM ($n = 6$/group). Boldface, italicized *P* values, and asterisks indicate significant differences between genotypes.

Because *Phd2* deficiency in the model presented in this study stabilizes both HIFα isoforms, we attempted to dissect the role of different HIFα isoforms in adipocyte function in vivo. Therefore, aP2-*Hif1α*KO or aP2-*Hif2α*KO mice were analyzed. Chow-fed aP2-*Hif1α*KO or aP2-*Hif2α*KO were comparable to control littermates (data not shown); therefore, these mice were analyzed after 12 weeks exposure to high-fat feeding. Notably, *Hif1α*-deleted mice manifested reduced BW gain and improved glucose tolerance on high-fat diet (Supplementary Fig. 4*A*–*C*). In contrast, adipose tissue *Hif2*-deleted mice fed a high-fat diet gained similar BW (Supplementary Fig. 4*D*) but showed worsening of glucose tolerance (Supplementary Fig. 4*E*) and elevated fasting insulin (Supplementary Fig. 4*F*), suggesting insulin resistance. There was no difference in plasma fasting NEFA or liver triglyceride levels in aP2-*Hif2α*KO or aP2-*Hif2α*KO mice compared with their littermate controls (Supplementary Table 1).

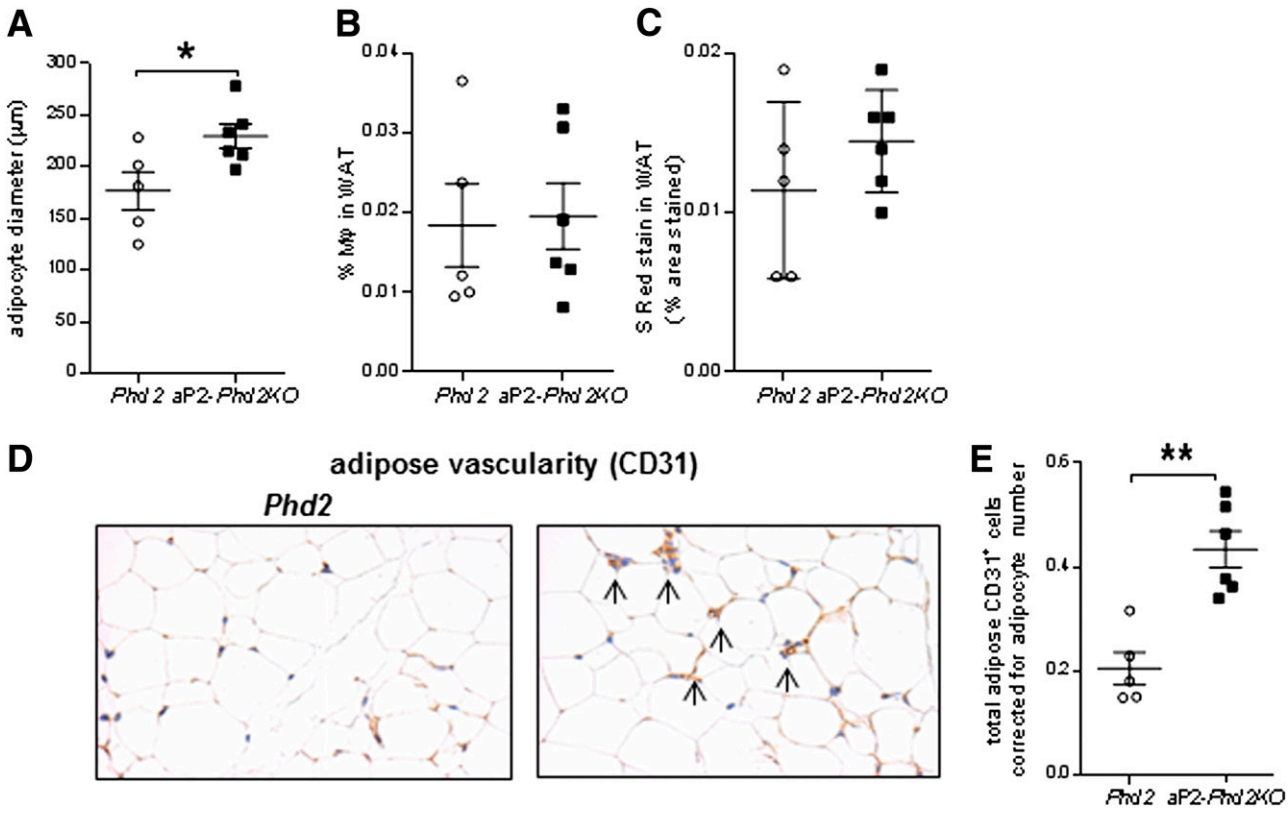

Figure 4—Adipose *Phd2* deficiency increases adipocyte size in parallel with increased adipose vasculature. *A*: Bigger adipocytes in aP2-*Phd2*KO mice (black squares; $n = 6$) compared with control littermates (open circles; $n = 5$). *B*: Similar macrophage numbers (F4/80-positive stained) in adipose tissue of aP2-*Phd2*KO mice. *C*: Similar total collagen deposition (Picrosirius Red [S Red] staining) in aP2-*Phd2*KO adipose. *D*: aP2-*Phd2*KO adipose tissue has more CD31-positive cells and vessels (arrows). *E*: Quantification of total vessel number corrected for adipocyte number. Original magnification ×200. $^*P < 0.05$, $^{**}P < 0.01$ between genotypes. WAT, white adipose tissue.

Adipose *Phd2* Deficiency Leads to Suppression of Lipolytic Signaling

To investigate the mechanism by which adipose *Phd2* deficiency drives adipocyte hypertrophy, we assessed lipolytic responses of the adipocytes in vitro under normoxic (21% O_2) and hypoxic (1% O_2) conditions. In normoxia, basal and β-adrenergic–stimulated NEFA release into the medium of aP2-*Phd2*KO adipocytes was significantly lower than control (Fig. 5*A*). The reduced lipolytic response of aP2-*Phd2*KO adipocytes was also apparent under hypoxic conditions; hypoxia itself attenuated stimulated but not basal lipolysis (Fig. 5*A*). The reduced NEFA release from *Phd2*-deficient adipocytes was associated with reduced levels of the key lipolytic proteins HSL and perilipin (Fig. 5*B*, *C*, and *E*). Lower HSL mRNA was also observed in aP2-*Phd2*KO adipose tissue, whereas perilipin mRNA levels were unaltered (Fig. 5*G*). In contrast, the mRNA of the triglyceride synthesis gene diacyglycerol acylotransferase-1 (*Dgat1*) was higher in aP2-*Phd2*KO adipose tissue. Supporting the HIF-1α dependence of this effect, adipocytes from aP2-*Hif1α*KO and not aP2-*Hif2α*KO mice showed a higher basal and β-adrenergic–stimulated NEFA release in hypoxia (Fig. 5*H*) as well as higher total HSL and perilipin protein levels (Fig. 5*I* and *J* and quantification in Supplementary Fig. 5*A–C*). Consistent with this, *Hif2*α-deficient adipocytes showed normal NEFA release and HSL levels (Supplementary Fig. 6*A–C*). Short-term activation of HSL is mediated by phosphorylation at serine 660 (protein kinase A mediated) and serine 565 (AMPK mediated) (42). Immunoblotting revealed that PHD/HIF-1α affected total HSL protein levels but not the p-HSL/total HSL protein ratio (Fig. 5*D* and *F* and Supplementary Fig. 5*C*). In addition, *Phd2* deficiency increased expression of the main antilipolytic α2-adrenergic receptor and tended to decrease levels of the lipolytic β3-adrenergic receptor, consistent with greater antilipolytic tone in aP2-*Phd2*KO adipose tissue (Fig. 5*G*).

Pharmacological Inhibition of HIF-PHD Suppresses Murine and Human Adipocyte Lipolysis

We next explored the effect on lipolysis of a small-molecule PHI that activates HIFα robustly (40,41). Pharmacological inhibition of PHDs in mouse adipocytes by PHI led to a significant stabilization of HIF-1α protein levels (10-fold; $P = 0.026$) and, to a lesser extent, HIF-2α (Fig. 6*A*). In both murine (Fig. 6*B*) and human (Fig. 6*C*) primary adipocytes, PHI elicited a profound suppression

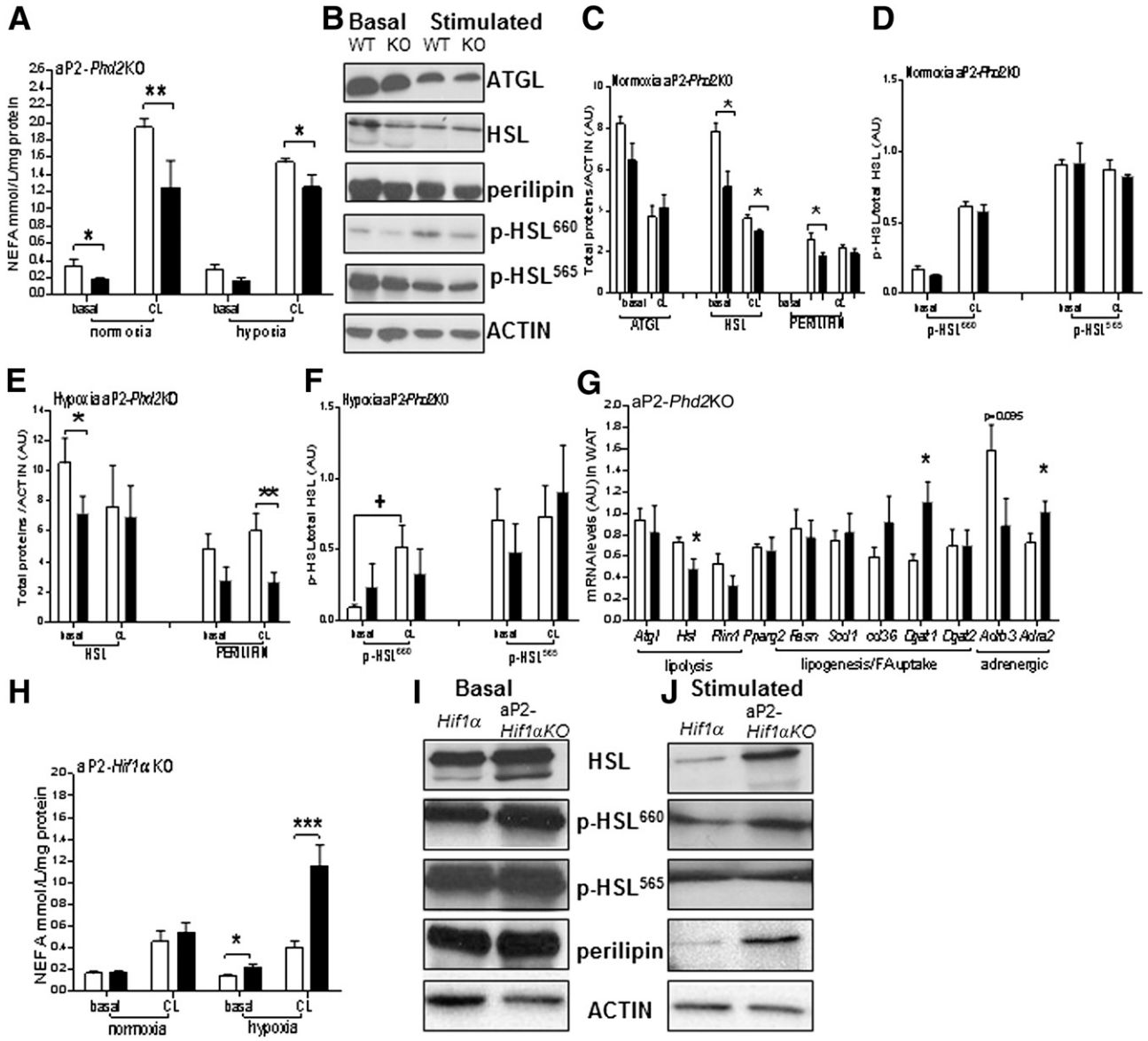

Figure 5—*Phd2* deficiency suppresses adipocyte lipolysis in vitro. *A*: NEFA release in aP2-*Phd2*KO isolated adipocytes cultured in normoxia (21% O_2) or hypoxia (1% O_2) and stimulated with CL316,243 (CL; 100 nmol/L) for 4 h show reduced lipolytic responses in both normoxia and hypoxia (n = 4/group). Induction by CL treatment was significant but has been omitted for clarity. *B*: Representative immunoblots of total ATGL, HSL, perilipin, and p-HSL at serine 660 and 565 under basal and CL316,243 stimulation in normoxia. Labeling on blots: wild-type (WT); *Phd2* and knockout (KO); and aP2-*Phd2*KO. *C*: Quantification (n = 3/group) of immunoblots for total ATGL, HSL, and perilipin levels corrected for β-actin in normoxia. *D*: Level of p-HSL corrected for total HSL in normoxia. Quantification of total HSL and perilipin proteins (*E*) and p-HSLs (*F*) in hypoxia. *G*: mRNA levels of key genes involved in the regulation of the adipocyte lipolytic response, patatin-like phospholipase domain containing 2 (*Atgl*), *Hsl*, perilipin 1 (*Plin1*), lipogenesis/fatty acid (FA) uptake peroxisome proliferator-activated receptor γ-2 (*Pparg2*), fatty acid synthase (*Fasn*), stearoyl-CoA desaturase (*Scd1*), fatty acid translocase (*cd36*), *Dgat1* and *Dgat2* and adrenergic signaling, β3-adrenergic receptor (*Adrb3*), and α2-adrenergic receptor (*Adra2*) were measured in adipose tissue of aP2-*Phd2*KO mice (black bars; n = 6/group) compared with control *Phd2* littermates (white bars; n = 6/group). *H*: NEFA release in the medium of aP2-*Hif1α*KO adipocytes (black bars) cultured in normoxia (21% O_2) or hypoxia (1% O_2) and stimulated with CL316,243 show increased lipolytic response in hypoxia (n = 4/group). Representative immunoblots of HSL, perilipin, and p-HSL at serine 660 and 565 (*I*) basal- and (*J*) CL316,243-stimulated lipolysis during hypoxia. $^*P < 0.05$, $^{**}P < 0.01$, $^{***}P < 0.001$ comparisons between genotypes within treatment; $+P < 0.05$ indicates significant induction of p-HSL^{660} after CL316,243 stimulation in the control *Phd2* but not in the aP2-*Phd2*KO adipocytes.

of basal and adrenergic agonist–stimulated NEFA release in normoxia. As was observed in aP2-*Phd2*KO, total ATGL was not affected, but HSL and perilipin protein levels were lower in the PHI-treated adipocytes (Fig. 6*D* and *E*) with no effect on the ratio of p-HSL to total HSL (Fig. 6*D*) after adrenergic stimulation. PHI treatment reduced basal ATGL levels (Fig. 6*F*).

Administration of PHI to mice in vivo suppressed basal plasma NEFA and β-adrenergic–stimulated NEFA release (Fig. 6*G*). This effect was consistent with a

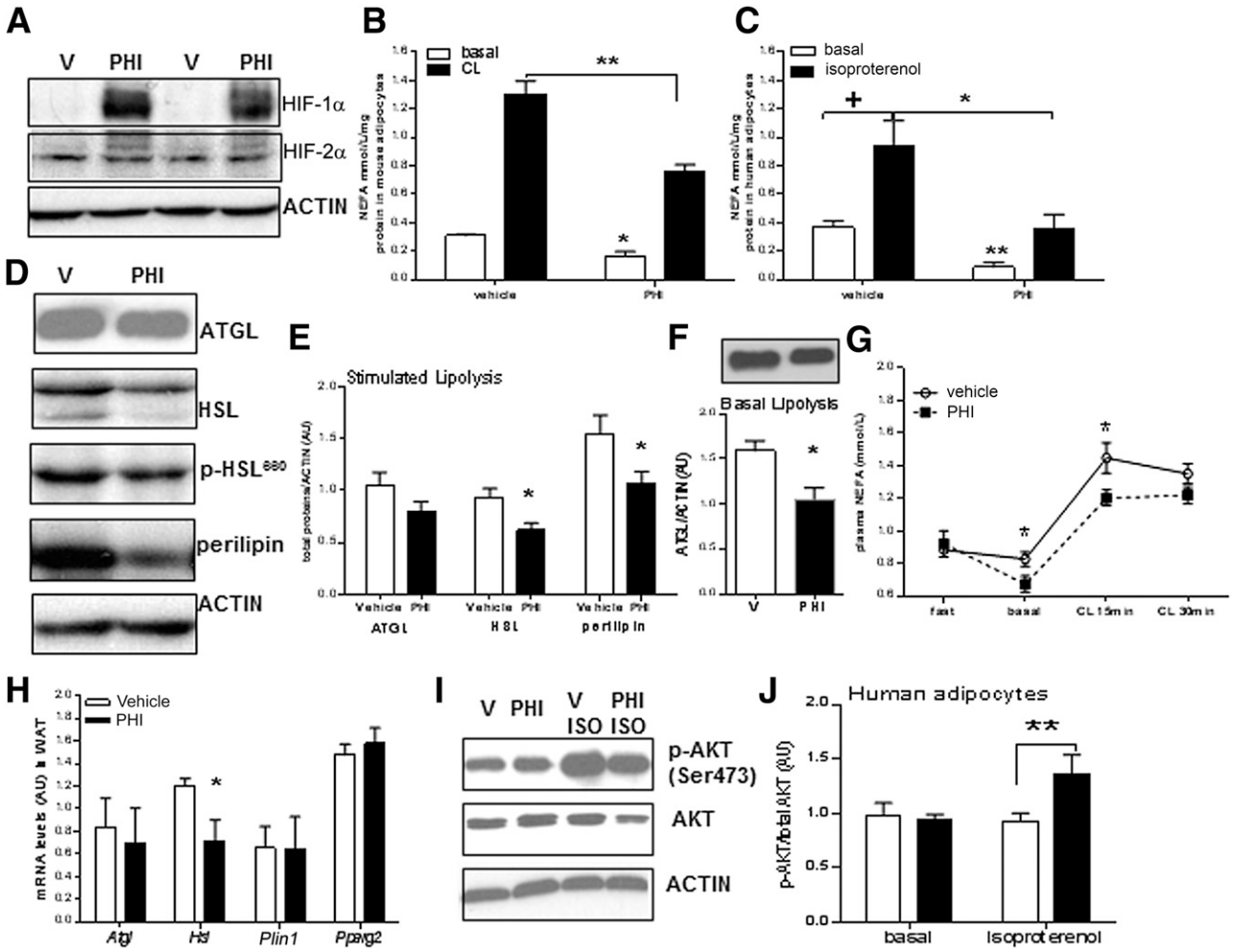

Figure 6—Pharmacological inhibition of HIF-PHD suppresses murine and human adipocyte lipolysis. Primary mouse (n = 4/group) and human adipocytes (n = 4/group) were pretreated with a selective PHI (0.5 mmol/L) or vehicle (V; DMSO, 0.5%) for 1 h prior to a standard β-adrenergic stimulation of lipolysis by CL316,243 (CL; 100 nmol/L) or isoproterenol (100 nmol/L) for 3 h. Medium was collected for measuring NEFA concentrations, and adipocytes were lysed for protein quantification and immunoblot analysis. *A*: Representative blot shows significant stabilization of HIF-1α levels and, to a lesser extent, HIF-2α levels by PHI in mouse adipocytes (n = 3/group) in normoxia. *B*: Reduced basal and CL-stimulated NEFA release in PHI pretreated mouse adipocytes. *C*: Reduced basal- and isoproterenol-stimulated NEFA release in PHI-pretreated human adipocytes. Representative mouse adipocyte immunoblots (*D*) and quantification graph (*E*) show unaltered ATGL but reduced HSL and perilipin levels after PHI treatment (n = 3/group) in stimulated lipolysis. *F*: Note that ATGL is reduced by PHI in basal lipolysis. *G*: In vivo administration of PHI i.p. (30 mg/kg BW) 1 h prior to CL i.p. (1 μg/g BW) in C57BL/6J mice caused reduction of NEFA release compared with vehicle-treated (5% DMSO) mice and a reduced lipolytic response after CL administration (n = 6/group). *H*: mRNA levels of key lipolytic genes (corrected for 18S levels) in adipose tissue of C57BL/6J administered PHI i.p. (30 mg/kg BW; black bars) 1 h prior to CL316,243 i.p. (1 μg/g BW) or vehicle-treated (5% DMSO; white bars) mice administration (n = 6/group). Immunoblots (*I*) and quantification graph (*J*) of p-AKT(Ser473), total AKT, and actin in human primary adipocytes pretreated with PHI basally and after isoproterenol (ISO) stimulation (n = 3/group). $^*P < 0.05$, $^{**}P < 0.01$, comparisons between PHI and V basally or after β-adrenergic stimulation; $+P < 0.05$ indicates that in human adipocytes, only the vehicle group showed significant NEFA release after isoproterenol; the PHI group showed a blunted response. WAT, white adipose tissue.

selective downregulation of HSL mRNA levels in adipose tissues from PHI-treated C57BL/6J mice (Fig. 6*H*). In human adipocytes in vitro, isoproterenol increased the phosphorylation of AKT (Ser473) in both vehicle and PHI-treated adipocytes (Fig. 6*I*). However, the ratio of p-AKT (Ser473) to total AKT was higher in the PHI-treated human adipocytes (Fig. 6*J*), suggesting selective enhancement of insulin sensitivity with PHD inhibition.

Adipose *PHD2* mRNA Levels Correlate With mRNA Levels of Lipolytic Genes in a Depot-Specific Manner in Humans

We further extended our findings on the role of PHD2 in adipose tissue in a cohort of patients with type 2 diabetes. Adipose *PHD2* (*EGLN1*) mRNA levels did not correlate with crude measures of obesity (BMI; Table 2). However, *PHD2* mRNA levels positively correlated with mRNA for caveolin (*CAV1*), a coactivator of the lipolytic protein

Table 2—PHD2 (EGLN1) correlations with genes involved in the lipolytic machinery in human SAT and VAT adipose depots

	Nondiabetic participants	Type 2 diabetic participants	*P* value
N	73	29	
Age (years)	47.23 ± 12.1	47.55 ± 11.3	0.9
BMI (kg/m^2)	37.7 ± 11.3	41.6 ± 6.8	0.09
Fasting glucose (mg/dL)	93.01 ± 12.7	163.2 ± 59.8	**<0.0001**
EGLN1 (RU) in SAT	0.084 ± 0.021	0.070 ± 0.016	**0.002**
EGLN1 (RU) in VAT	0.082 ± 0.019	0.079 ± 0.020	0.4

	All participants		Nondiabetic participants		Type 2 diabetic participants	
	r	*P* value	*r*	*P* value	*r*	*P* value
SAT						
Age (years)	−0.056	0.5	−0.047	0.7	0.046	0.8
BMI (kg/m^2)	0.013	0.9	−0.001	0.9	−0.03	0.9
Fasting glucose (mg/dL)	−0.13	0.2	−0.015	0.9	0.17	0.3
CAV1 (RU)	0.47	**<0.0001**	0.46	**<0.0001**	0.46	**0.03**
ABHD5 (RU)	0.32	**0.01**	0.34	0.08	0.11	0.6
AKAP (RU)	0.32	**0.01**	0.36	0.06	0.55	**0.01**
ATGL (RU)	0.10	0.4	−0.10	0.5	0.12	0.6
MGLL (RU)	0.14	0.2	0.13	0.4	0.03	0.9
PRKACA (RU)	0.15	0.2	−0.11	0.4	0.68	**0.001**
PLIN1 (RU)	−0.15	0.2	−0.36	**0.04**	0.16	0.4
CIDEC (RU)	−0.01	0.9	−0.12	0.4	0.12	0.5
TIP47 (RU)	−0.27	**0.04**	−0.25	0.1	−0.14	0.5
VAT						
Age (years)	−0.05	0.6	0.01	0.9	−0.17	0.3
BMI (kg/m^2)	−0.08	0.4	−0.06	0.5	−0.16	0.3
Fasting glucose (mg/dL)	0.03	0.7	0.11	0.3	0.03	0.8
CAV1 (RU)	0.12	0.3	0.13	0.3	0.24	0.3
ABHD5 (RU)	0.07	0.6	−0.05	0.8	0.36	0.2
AKAP (RU)	0.07	0.5	0.01	0.9	0.21	0.4
ATGL (RU)	0.07	0.5	0.10	0.5	−0.01	0.9
MGLL (RU)	0.38	**0.004**	0.42	**0.008**	0.17	0.5
PRKACA (RU)	−0.06	0.6	−0.06	0.6	−0.12	0.6
PLIN1 (RU)	0.17	0.2	0.21	0.2	0.19	0.4
CIDEC (RU)	0.09	0.4	0.045	0.7	0.18	0.4
TIP47 (RU)	0.11	0.3	−0.02	0.9	0.38	0.1

RU, relative units; VAT, visceral adipose tissue. Boldface indicates significant *P* values.

ATGL, *ABHD5*, and another lipolytic cascade-modulating gene, the a-kinase anchoring protein (*AKAP*). Notably, type 2 patients with diabetes had lower SAT *PHD2* mRNA levels than nondiabetic participants (Table 2).

DISCUSSION

In this study, we describe a novel biological role for pseudohypoxia (Fig. 7) in the suppression of adipocyte lipolysis. Genetic *Phd2* deficiency resulted in an increased adipose mass, but with normal glucose tolerance and reduced circulating levels of fatty acids. This apparently protective adipose expansion was associated with increased vascularity and no increase in adipose tissue macrophage burden or fibrosis. Mechanistic dissection revealed that in isolated mouse adipocytes in vitro, basal and β-adrenergic–stimulated release of NEFA was reduced by genetic inactivation of *Phd2*. Importantly, these findings were recapitulated by the acute exposure of mouse and human adipocytes to a selective PHI that targets PHD2.

In oxygenated cells, the HIF-PHD promote degradation of HIFα subunits following association of hydroxylated HIF with the VHL ubiquitin E3 ligase. PHD2 is the most abundant of these enzymes and the most important in setting levels of HIF activity in normoxic cells (20). Thus, PHD2 inactivation by genetic or pharmacological means is predicted to mimic hypoxia, creating a pseudohypoxic signal that activates the HIF transcriptional cascade in normoxic conditions. Although we cannot be certain that all of the effects we observed were mediated by this mechanism, several lines of evidence support this. First, both HIFα proteins and HIF transcriptional target genes were induced in adipose tissues and cells by these interventions. Second, genetic inactivation of *Hif1α* revealed effects that were consistent with induction of HIF being responsible for at least some of the observed effects of *Phd2* inactivation. In particular, inactivation of *Hif1α* in adipose tissues resulted in reduced BW gain with high-fat feeding and enhanced lipolytic responses in adipocytes. We therefore propose a model in which

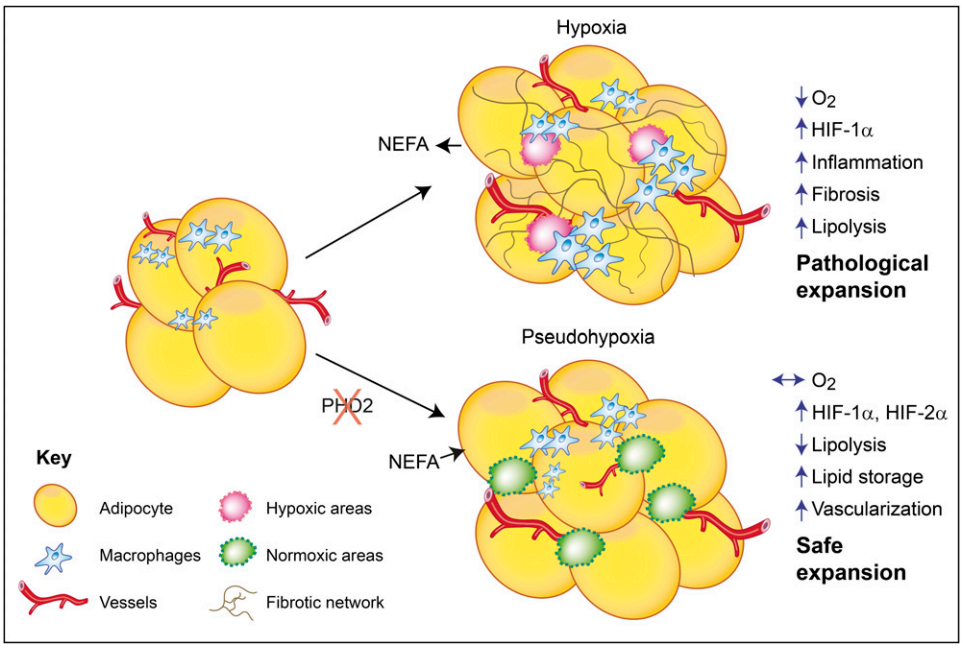

Figure 7—Schematic summary of the effects of pseudohypoxia in adipose tissue. During excessive fat accumulation in obesity (top panel), the adipose tissue vasculature fails to facilitate this expansion, and areas of hypoxia are created in adipose tissue (pink-shaded areas). This leads to activation of HIF-1α, recruitment of proinflammatory macrophages (light blue shapes), collagen deposition and fibrosis (thin brown lines), increased fatty acid release (lipolysis), ectopic fat deposition and insulin resistance, and pathological adipose expansion. In contrast, priming adipose tissue to be pseudohypoxic, by inhibiting the HIF-PHD (genetic PHD2 deletion or pharmacological PHD inhibition), stabilizes HIF-1α and HIF-2α. Adipose tissue expands due to reduced lipolysis and increased lipid storage, leading to reduced ectopic lipid deposition. This expansion does not alter the oxygen availability (green areas denote normoxia) in the tissue due to enhanced vascularization (red vessel shapes), thus leading to safe expansion without insulin resistance.

Phd2 inactivation leads to coordinated activation of HIF pathways including marked upregulation of *Vegfα* and *Angptl4* (most likely through HIF-2α activation) with concomitant suppression of the key lipolytic enzyme HSL and upregulation of lipogenesis through *Dgat1* to increase fat-cell lipid storage. We extended our findings to show a positive correlation between *PHD2* and *ABHD5* in SAT in humans. We also found a negative correlation between *PHD2* mRNA with mRNA for the lipid droplet protein-encoding genes perilipin or TIP47. These data support a role for oxygen sensing as an endogenous regulator of adipose tissue lipid mobilization in humans and suggest PHD2 inhibition could promote metabolically protective peripheral fat accumulation. In this regard, reduced adipose perilipin protein levels in the ap2-*Phd2*KO mouse model were an unexpected finding, as this might be predicted to promote lipolysis. The regulation of the lipolytic machinery is complex, and future work will investigate perilipin phosphorylation and indeed other lipid droplet protein levels that may reconcile the clearly antilipolytic effects of PHD inhibition at this functional level.

A number of observational studies have implicated adipose hypoxia in the pathogenesis of insulin-resistant obesity (2–4). Furthermore, several groups have generated transgenic mouse models of HIF-1α modulation in adipose tissue. Some (5,29–32), but not all (28,43,44), of these studies have reported that elevated levels of HIF-1α lead to obesity, with fibrotic scarring and insulin resistance in the adipose tissue. Consistent with this, genetic inactivation or pharmacological inhibition of the HIF system is protective against obesity and its associated metabolic abnormalities (32,33). Surprisingly, overexpression of HIF-1α specifically in adipose tissue did not induce canonical HIF-target genes (*Vegfα* and *Glut1*) or affect the local adipose tissue angiogenic phenotype (5). Instead, HIF-1α overexpression caused a profibrotic adipose gene expression profile with associated histological abnormalities (5). These contrasting findings may reflect context-dependent regulation of overlapping target genes by the pleiotropic HIFs. Underlining this complexity, a recent study showed no obvious phenotypic changes under normal dietary conditions with an adipose-selective *Phd2* deletion mouse model analogous to ours (43). Indeed, this study reported obesity resistance in adipose *Phd2*-deleted mice (43) in contrast to previous reports showing HIF-1α activation leads to an obese phenotype (5,29–32). Moreover, obesity resistance in the adipose-selective *Phd2*-deleted mice became apparent only after chronic high-fat feeding (43). The reasons for the discrepancy between these studies could reflect differences in mouse strain genetic background, age, dietary intervention, and the level of *Phd2* deletion achieved. Moreover, we did not observe a compensatory Phd3 upregulation in our ap2-*Phd2*KO model, in contrast to Matsuura et al. (43). Finally, while this

manuscript was in revision, another study using a hypomorphic *Phd2* mutant mouse model of whole-animal PHD2 deficiency showed an improved metabolic profile with reduced adiposity (44). Complementary findings between our study and that of Rahtu-Korpela et al. (44) are promising in terms of the therapeutic potential of PHIs to improve cholesterol as well as reduced plasma NEFA levels (our study) and differences in adiposity phenotypes likely reflect our distinct tissue-specific effects versus those of whole-animal *Phd2* hypomorphicity. In any case, the focus of the work presented in this study is the effect of PHD/HIF signaling on adipocytes in mice and humans under normal dietary conditions and not under obesogenic conditions. Indeed, we have shown high-fat diets regulate the PHD system (7) and thus may potentially confound important baseline differences.

Of note, enlarged adipocytes but normal glucose tolerance test responses were reported in a distinct genetic mouse model of adipose-specific HIFα activation caused by ablation of the VHL tumor suppressor (a factor degrading HIF downstream of PHD action) (45). The adipose-specific VHL knockout model exhibited a cardiac hypertrophy phenotype resulting from severe adipose inflammation and highlighted the effect of manipulating distinct HIFα isoform levels (45). We show that targeting PHDs, as opposed to VHL, also reveals distinct effects, and our findings are key in order to fully evaluate which components of the HIF signaling pathway are relevant to metabolic pathologies.

The pseudohypoxic induction of HIF caused by *Phd2* deletion may effectively pre-empt the remodeling effects normally caused by local hypoxia when fat rapidly expands in obesity. This may prime adipose tissue to resist the inflammatory and fibrotic responses seen with vascular rarefaction in obesity by activating the proangiogenic factors such as *Angptl4* and *Vegfα* and coordinating more effective vascular remodeling to cope with fat deposition (5,30,32). Inactivation of *Phd2* better mimics the coordinated physiological activation of all isoforms of HIF system than overexpression of a single isoform. Thus, although in many cells, PHD2 has greater activity on HIF-1α than HIF-2α (46), we observed that inactivation of *Phd2* deficiency in adipose tissue is also associated with stabilization of HIF-2α. A large body of data now indicates that HIF-1α and HIF-2α have different, and sometimes opposing, biological effects (47). In keeping with this, we observed entirely different responses to the inactivation of HIF-1α and HIF-2α in adipose tissues. Although inactivation of HIF-2α did not result in altered adipose mass under the experimental conditions used, this does not preclude concurrent activation of HIF-2α contributing to the phenotype associated with *Phd2* deficiency. Indeed, HIF-2α is most likely involved in the proangiogenic response of aP2-*Phd2*KO mice. It is also possible that quantitative differences in the extent of HIF pathway activation underlie the differences in adipose phenotypes, as has been observed in the heart (45,48) and pancreatic β-cell (49,50), where pronounced induction of HIF is associated with organ dysfunction, but modest induction has beneficial effects on metabolic function or protection from ischemia.

Our work reveals a novel role for the oxygen sensor PHD2 in the regulation of adipocyte lipolysis. PHD2 inhibition suppresses lipolysis and promotes angiogenic responses through distinct HIF isoform activation, thereby promoting benign adipose tissue expansion. Notably, PHIs similar to those used in this study are under clinical trials for anemia and ischemia (33,34). Although the effects of PHD inhibition in metabolic disease remain to be tested, our data suggest that selective PHD2 inhibition may also be beneficial for ameliorating the detrimental metabolic consequences of elevated fatty acid levels found in insulin-resistant obesity and lipodystrophic dyslipidemia.

Acknowledgments. The authors thank Tammie Bishop and Ya-Min Tian (Ratcliffe Laboratory, Oxford, U.K.) for advice on the use of PHIs; Xantong Zou, Rhona Aird, and Karen French for excellent technical assistance; and the staff in the biomedical research resources facility (Edinburgh) for maintenance of the mouse colony. The authors also thank Prof. Nicholas Hastie, Prof. Stewart Forbes, and Prof. John Iredale (Edinburgh) for useful discussions.

Funding. This work was supported by a Sir Henry Wellcome Postdoctoral Fellowship (to Z.M., 085458/Z/08/Z) and a British Heart Foundation/University of Edinburgh Centre of Research Excellence Transition Award Fellowship (to Z.M.).

Duality of Interest. C.J.S. and P.J.R. are scientific cofounders and hold equity in ReOx Ltd., a company that is seeking to develop HIF hydroxylase inhibitors for therapeutic use. No other potential conflicts of interest relevant to this article were reported.

Author Contributions. Z.M. designed, performed experiments, analyzed data, and wrote the manuscript. N.M.M. designed, performed experiments, contributed to discussion, and reviewed and edited the manuscript. J.M.M.N. and J.M.F.-R. designed, performed, and analyzed the human diabetic cohort gene expression study. C.C.W. and K.J.S. provided the human adipose biopsies. C.J.S. provided essential reagents and reviewed and edited the manuscript. J.R.S. contributed to discussion and reviewed and edited the manuscript. P.J.R. provided the *Phd2* homofloxed mice, contributed to discussion, and reviewed and edited the manuscript. Z.M. is the guarantor of this work and, as such, had full access to all the data in the study and takes responsibility for the integrity of the data and the accuracy of the data analysis.

References

1. Pasarica M, Sereda OR, Redman LM, et al. Reduced adipose tissue oxygenation in human obesity: evidence for rarefaction, macrophage chemotaxis, and inflammation without an angiogenic response. Diabetes 2009;58:718–725

2. Gealekman O, Guseva N, Hartigan C, et al. Depot-specific differences and insufficient subcutaneous adipose tissue angiogenesis in human obesity. Circulation 2011;123:186–194

3. Trayhurn P, Wood IS. Adipokines: inflammation and the pleiotropic role of white adipose tissue. Br J Nutr 2004;92:347–355

4. Hosogai N, Fukuhara A, Oshima K, et al. Adipose tissue hypoxia in obesity and its impact on adipocytokine dysregulation. Diabetes 2007;56:901–911

5. Rausch ME, Weisberg S, Vardhana P, Tortoriello DV. Obesity in C57BL/6J mice is characterized by adipose tissue hypoxia and cytotoxic T-cell infiltration. Int J Obes (Lond) 2008;32:451–463

6. Halberg N, Khan T, Trujillo ME, et al. Hypoxia-inducible factor 1alpha induces fibrosis and insulin resistance in white adipose tissue. Mol Cell Biol 2009;29:4467–4483

7. Michailidou Z, Turban S, Miller E, et al. Increased angiogenesis protects against adipose hypoxia and fibrosis in metabolic disease-resistant 11β-hydroxysteroid dehydrogenase type 1 (HSD1)-deficient mice. J Biol Chem 2012; 287:4188–4197
8. Sun K, Wernstedt Asterholm I, Kusminski CM, et al. Dichotomous effects of VEGF-A on adipose tissue dysfunction. Proc Natl Acad Sci U S A 2012;109:5874–5879
9. Elias I, Franckhauser S, Ferré T, et al. Adipose tissue overexpression of vascular endothelial growth factor protects against diet-induced obesity and insulin resistance. Diabetes 2012;61:1801–1813
10. Sung HK, Doh KO, Son JE, et al. Adipose vascular endothelial growth factor regulates metabolic homeostasis through angiogenesis. Cell Metab 2013; 17:61–72
11. Virtue S, Vidal-Puig A. Adipose tissue expandability, lipotoxicity and the Metabolic Syndrome—an allostatic perspective. Biochim Biophys Acta 2010; 1801:338–349
12. Ebbert JO, Jensen MD. Fat depots, free fatty acids, and dyslipidemia. Nutrients 2013;5:498–508
13. Sun K, Kusminski CM, Scherer PE. Adipose tissue remodeling and obesity. J Clin Invest 2011;121:2094–2101
14. Rupnick MA, Panigrahy D, Zhang CY, et al. Adipose tissue mass can be regulated through the vasculature. Proc Natl Acad Sci U S A 2002;99:10730–10735
15. Hausman GJ, Richardson RL. Adipose tissue angiogenesis. J Anim Sci 2004;82:925–934
16. Cao Y. Angiogenesis modulates adipogenesis and obesity. J Clin Invest 2007;117:2362–2368
17. Semenza GL. Oxygen homeostasis. Wiley Interdiscip Rev Syst Biol Med 2010;2:336–361
18. Yun Z, Maecker HL, Johnson RS, Giaccia AJ. Inhibition of PPAR gamma 2 gene expression by the HIF-1-regulated gene DEC1/Stra13: a mechanism for regulation of adipogenesis by hypoxia. Dev Cell 2002;2:331–341
19. Shimba S, Wada T, Hara S, Tezuka M. EPAS1 promotes adipose differentiation in 3T3-L1 cells. J Biol Chem 2004;279:40946–40953
20. Ratcliffe PJ. Oxygen sensing and hypoxia signalling pathways in animals: the implications of physiology for cancer. J Physiol 2013;591:2027–2042
21. Bruick RK, McKnight SL. A conserved family of prolyl-4-hydroxylases that modify HIF. Science 2001;294:1337–1340
22. Epstein AC, Gleadle JM, McNeill LA, et al. C. elegans EGL-9 and mammalian homologs define a family of dioxygenases that regulate HIF by prolyl hydroxylation. Cell 2001;107:43–54
23. Ivan M, Kondo K, Yang H, et al. HIFalpha targeted for VHL-mediated destruction by proline hydroxylation: implications for O2 sensing. Science 2001;292:464–468
24. Jaakkola P, Mole DR, Tian YM, et al. Targeting of HIF-alpha to the von Hippel-Lindau ubiquitylation complex by O2-regulated prolyl hydroxylation. Science 2001;292:468–472
25. Floyd ZE, Kilroy G, Wu X, Gimble JM. Effects of prolyl hydroxylase inhibitors on adipogenesis and hypoxia inducible factor 1 alpha levels under normoxic conditions. J Cell Biochem 2007;101:1545–1557
26. Regazzetti C, Peraldi P, Grémeaux T, et al. Hypoxia decreases insulin signaling pathways in adipocytes. Diabetes 2009;58:95–103
27. Zhang X, Lam KS, Ye H, et al. Adipose tissue-specific inhibition of hypoxia-inducible factor 1α induces obesity and glucose intolerance by impeding energy expenditure in mice. J Biol Chem 2010;285:32869–32877
28. He Q, Gao Z, Yin J, Zhang J, Yun Z, Ye J. Regulation of HIF-1alpha activity in adipose tissue by obesity-associated factors: adipogenesis, insulin, and hypoxia. Am J Physiol Endocrinol Metab 2011;300:E877–E885
29. Jiang C, Qu A, Matsubara T, et al. Disruption of hypoxia-inducible factor 1 in adipocytes improves insulin sensitivity and decreases adiposity in high-fat diet-fed mice. Diabetes 2011;60:2484–2495
30. Lee KY, Gesta S, Boucher J, Wang XL, Kahn CR. The differential role of Hif1β/Arnt and the hypoxic response in adipose function, fibrosis, and inflammation. Cell Metab 2011;14:491–503
31. Krishnan J, Danzer C, Simka T, et al. Dietary obesity-associated Hif1α activation in adipocytes restricts fatty acid oxidation and energy expenditure via suppression of the Sirt2-NAD+ system. Genes Dev 2012;26:259–270
32. Sun K, Halberg N, Khan M, Magalang UJ, Scherer PE. Selective inhibition of hypoxia-inducible factor 1α ameliorates adipose tissue dysfunction. Mol Cell Biol 2013;33:904–917
33. Hewitson KS, McNeill LA, Schofield CJ. Modulating the hypoxia-inducible factor signaling pathway: applications from cardiovascular disease to cancer. Curr Pharm Des 2004;10:821–833
34. Fraisl P, Aragonés J, Carmeliet P. Inhibition of oxygen sensors as a therapeutic strategy for ischaemic and inflammatory disease. Nat Rev Drug Discov 2009;8:139–152
35. Mazzone M, Dettori D, Leite de Oliveira R, et al. Heterozygous deficiency of PHD2 restores tumor oxygenation and inhibits metastasis via endothelial normalization. Cell 2009;136:839–851
36. Ryan HE, Poloni M, McNulty W, et al. Hypoxia-inducible factor-1alpha is a positive factor in solid tumor growth. Cancer Res 2000;60:4010–4015
37. Gruber M, Hu CJ, Johnson RS, Brown EJ, Keith B, Simon MC. Acute postnatal ablation of Hif-2alpha results in anemia. Proc Natl Acad Sci U S A 2007; 104:2301–2306
38. He W, Barak Y, Hevener A, et al. Adipose-specific peroxisome proliferator-activated receptor gamma knockout causes insulin resistance in fat and liver but not in muscle. Proc Natl Acad Sci U S A 2003;100:15712–15717
39. Adam J, Hatipoglu E, O'Flaherty L, et al. Renal cyst formation in Fh1-deficient mice is independent of the Hif/Phd pathway: roles for fumarate in KEAP1 succination and Nrf2 signaling. Cancer Cell 2011;20:524–537
40. Tian YM, Yeoh KK, Lee MK, et al. Differential sensitivity of hypoxia inducible factor hydroxylation sites to hypoxia and hydroxylase inhibitors. J Biol Chem 2011;286:13041–13051
41. Bishop T, Talbot NP, Turner PJ, et al. Carotid body hyperplasia and enhanced ventilatory responses to hypoxia in mice with heterozygous deficiency of PHD2. J Physiol 2013;591:3565–3577
42. Girousse A, Langin D. Adipocyte lipases and lipid droplet-associated proteins: insight from transgenic mouse models. Int J Obes (Lond) 2012;36:581–594
43. Matsuura H, Ichiki T, Inoue E, et al. Prolyl hydroxylase domain protein 2 plays a critical role in diet-induced obesity and glucose intolerance. Circulation 2013;127:2078–2087
44. Rahtu-Korpela L, Karsikas S, Hörkkö S, et al. HIF prolyl 4-hydroxylase-2 inhibition improves glucose and lipid metabolism and protects against obesity and metabolic dysfunction. Diabetes 1 May 2014 [Epub ahead of print]
45. Lin Q, Huang Y, Booth CJ, et al. Activation of hypoxia-inducible factor-2 in adipocytes results in pathological cardiac hypertrophy. J Am Heart Assoc 2013;2: e000548
46. Huang J, Zhao Q, Mooney SM, Lee FS. Sequence determinants in hypoxia-inducible factor-1alpha for hydroxylation by the prolyl hydroxylases PHD1, PHD2, and PHD3. J Biol Chem 2002;277:39792–39800
47. Keith B, Johnson RS, Simon MC. HIF1α and HIF2α: sibling rivalry in hypoxic tumour growth and progression. Nat Rev Cancer 2012;12:9–22
48. Kerkelä R, Karsikas S, Szabo Z, et al. Activation of hypoxia response in endothelial cells contributes to ischemic cardioprotection. Mol Cell Biol 2013;33: 3321–3329
49. Cantley J, Selman C, Shukla D, et al. Deletion of the von Hippel-Lindau gene in pancreatic beta cells impairs glucose homeostasis in mice. J Clin Invest 2009; 119:125–135
50. Cheng K, Ho K, Stokes R, et al. Hypoxia-inducible factor-1alpha regulates beta cell function in mouse and human islets. J Clin Invest 2010;120:2171–2183